ELSEVIER

Polymer 41 (2000) 5415–5421

polymer

Deformation processes in high impact polystyrene as revealed by analysis of arrested cracks

L. Rios-Guerrero, H. Keskkula, D.R. Paul*

Department of Chemical Engineering and Texas Materials Institute University of Texas at Austin, Austin, TX 78712, USA

Received 22 March 1999; received in revised form 24 September 1999; accepted 27 September 1999

Abstract

Fracture of rubber-toughened polystyrene (HIPS) has been studied via post-mortem analysis of specimens with arrested cracks formed under impact loading conditions. This methodology involves the study of the deformed region around an arrested crack tip by electron microscopy. It was applied to two commercial HIPS products and two experimental products with sub-micron rubber particles. For the HIPS materials, the arrested crack tip has a blunted shape with a width from 50 to 100 μm depending of the material and its impact resistance. As expected, massive crazing was found in all these materials around the crack. In a narrow zone just ahead of the crack tip, where the crack would have continued to grow if not arrested, considerable elongation and deformation of the rubber particles was observed. This zone appears to be the precursor of the crack. In this region, "dilatation" and "shear" bands of more than 50 μm long were observed. Higher magnification TEM observations show highly deformed rubber particles ("S" or "tear-drop" shape) along the shear bands of 1–6 μm width. Three different kind of cavitation was observed just ahead of the crack tip: (1) small voids inside the membranes of the rubber particles; (2) large voids in the interface between rubber particles and the matrix and (3) interfacial cavities within the particles between the rubber membrane and the polystyrene occlusions. Within the narrow shear-bands there is evidence of shear yielding in the fracture of HIPS, similar to that observed in more ductile polymers.

Keywords: Deformation; High impact polystyrene; Arrested cracks

1. Introduction

Bucknall [1] proposed in the mid-1970s that toughness enhancement of rubber-modified brittle polymer matrices is due to the generation and efficient termination of crazes by the rubber particles, i.e. the theory of multiple crazing. Thus, the impact energy of high impact polystyrene (HIPS) may be attributed to the energy required to form an extensive network of crazes [2,3]. It has been argued that the efficiency of the rubber phase to produce and stop crazes must be a function of the rubber particle size [4–9]. However, several recent studies [10–19] have suggested that the process of plastic deformation of HIPS is more complex. Based on real-time small angle X-ray scattering studies, Bubeck et al. [10] and Magalhaes et al. [14] reported evidence that crazing accounts for about a half of the total plastic strain in HIPS and the strain due to non-crazing mechanisms occurs before that due to crazing mechanisms. According to recent theoretical analysis and modeling of cavitation [11–13,15,16,19] the rubber particles in a toughened plastic are constrained by the surrounding matrix and are subjected to substantial triaxial tensile stresses. This strain is sufficient to produce cohesive failure in the rubber (cavitation). A rubber particle may cavitate thereby lowering the inner hydrostatic pressure and inducing a micro-shear band in the surrounding matrix; but no direct experimental evidence has been reported for brittle matrices like polystyrene. In HIPS the cavitation process is complex, because it might be a combination of the development of small voids within the rubber membranes of the "salami" particles or interface failure, both external and internal, i.e. between the rubber membrane and the polystyrene matrix and occlusions. It would be very important to experimentally determine the voiding sequence in high-speed fracture of HIPS and to determine if the cavitation process is associated with the formation of shear-bands in the polystyrene matrix.

Recent work [20–26] in a number of laboratories including our own have shown the value of post-mortem analysis by transmission electron microscopy (TEM) in the region around an arrested crack to learn about deformation mechanisms, particularly toughened semi-ductile engineering thermoplastics. Similarly, we believe that

* Corresponding author. Tel.: +1-512-471-5392; fax: +1-512-471-0542.
E-mail address: drp@che.utexas.edu (D.R. Paul).

0032-3861/00/$ - see front matter
PII: S0032-3861(99)00725-9

Table 1
Physicochemical characterization

Code	Rubber type	Rubber content (wt%)	$\bar{d}_w$ (μm)	$\bar{M}_n$	$\bar{M}_w$	$\bar{M}_z$	Swelling index[a]	Gel (wt. %)[a]
HIPS A	Unknown	8[b]	2.5	69,000	157,000	288,000	10.6	39.8
HIPS B	Taketene 1202	8	1.5	80,000	210,000	398,000	9.8	20.7
HIPS C	Solprene 255	6	0.6	77,000	342,000	817,000	10.2	32.6
HIPS D	Solprene 255	6	0.7	140,000	254,000	421,000	15.3	13.6

[a] Determined in toluene.
[b] An estimate.

such post-mortem analysis of specimens fractured under impact test conditions can provide some insights about the deformation mechanisms of rubber-toughened brittle polymers. The objective of this paper is to report the results from application of this methodology to four rubber-toughened polystyrenes with different properties and particle sizes. Analysis of the plastic zone right ahead of the crack tip by TEM and SEM provides direct experimental evidence of a narrow zone of shear yielding in HIPS. Subsequent papers will report results for rubber-toughened styrene–methyl methacrylate copolymers with different rubber types.

2. Materials preparation and characterization

Relevant characteristics of the materials used in this study are given in Table 1. The study included two commercial samples of rubber-modified polystyrenes with weight average particle size, $\bar{d}_w$, of 2.5 μm (Dow 482) and 1.5 μm (Resirene 6220) plus two laboratory samples with sub-micron rubber particles size, $\bar{d}_w = 0.6$ μm (made by a mass-suspension process) and $\bar{d}_w = 0.7$ μm (made by a mass-casting process). The laboratory products were made with a commercial polybutadiene rubber specially designed for polystyrene modification, Solprene 255. To prepare these materials, the rubber was dissolved in styrene at 80°C, using an anchor impeller (60 rpm) until a transparent and gel-free solution was obtained.

2.1. Suspension polymerization process

A mass polymerization up to 30% conversion was carried out using 1,1 bis(*tert*-butyl peroxy)cyclohexane as initiator (6.6 g for 13.8 kg of styrene) in a pilot plant reactor (10 gallons). The temperature was controlled at 115°C. The reactor was equipped with two impellers for high shearing agitation (anchor at the bottom and a turbine, 4-blades at 45°, in an adjustable upper position) in order to generate sub-micron rubber particles. The reaction time was about 60 min. Subsequent polymerization to more than 99% conversion was carried out in suspension polymerization, adding hot water (17 kg) with polyacrylic acid (Acrystab from Tecvinsa Co., 0.2 wt%) as suspension agent. Additional 1,1 bis(*tert*-butyl peroxy)cyclohexane (93.2 g) and antioxidant, Irganox 1076 (7 g), dissolved in 300 ml of styrene, were fed into the reactor vessel from the beginning of this second step. Reaction temperature was controlled at 120°C for 5 h. The monomer/water ratio was about 0.8.

2.2. Casting polymerization process

First, a mass polymerization to 30% conversion was carried out at 85°C for 90 min using benzoyl peroxide as initiator (0.5 g/kg styrene) in a glass reactor (2 l) equipped with an anchor impeller (200 rpm). Subsequent polymerization (with additional benzoyl peroxide and Irganox 1076) was carried out in a closed-glass casting mold placed in an oven at 90°C for 9 h. The total volatile content of the product, determined by gas chromatography (with a headspace injector), revealed the final conversion to be 99% for both systems.

An image analyzer (Opto-photo) program was used for to determine the particle size distribution for each HIPS from several TEM photomicrographs. More than 100 particles were measured to calculate the number ($\bar{d}_n$) and weight ($\bar{d}_w$) average rubber particle diameters. The soluble and gel fractions were separated from a 2 wt% toluene dispersion by ultracentrifugation. The molecular weight of the soluble fraction was determined using a GPCWaters Millennium 2010 by polystyrene standards with tetrahydrofuran as the solvent. The gel content, swelling index (SI), molecular weight and the average rubber particle size ($\bar{d}_w$) are listed in Table 1. The average molecular weights obtained are quite similar for HIPS samples A, B and D; however, HIPS C has a very high value for $M_z(817 \times 10^3)$.

The swelling index is an indirect measure of the degree of crosslinking of the rubbery phase (the higher the SI, the lower the crosslinking degree). The laboratory mass-casting process of HIPS D gives the lowest crosslinking level ($SI = 15.3$), in comparison with commercial HIPS A and B, which have much lower swelling indexes of about 10. The low reaction-temperature (90°C) of the mass-casting process gives rise to a lower crosslinking level of the rubber in HIPS D.

For the same rubber content, the higher the rubber phase volume fraction (RPVF), the higher the gel fraction. HIPS A and HIPS B have similar weight percent of rubber, but they clearly have significant by different rubber phase fractions, 39.8% vs. 20.7%, respectively (Table 1). Also the difference

Table 2
Tensile and impact characterization

Material	Izod strength (J/m)	Yield stress (MPa)	Yield strain (%)	Stress at break (MPa)	Strain at break (%)	Tensile modulus (GPa)
HIPS A[a]	141	14	1.34	13.5	43.1	1.56
HIPS B[a]	85	27	1.29	23.5	44.7	2.15
HIPS C[a]	78	35	2.34	32.9	39.7	2.05
HIPS D	73	29	2.06	34.2	31.4	1.82

[a] Injection molded.

in the weight average rubber particle size, 2.5 μm vs. 1.5 μm indicates a more efficient use of the rubber in HIPS A. Similarly, mass-suspension HIPS D has very low average particle size ($\bar{d}_w = 0.7$ μm) corresponding to a lower rubber content (6 wt%) and low level of polystyrene occlusions. This low gel (13.6 wt%) for HIPS D may be due to some non-crosslinked rubber that might be dissolved in toluene, because the polymerization temperature (90°C) is quite low for thermal crosslinking. Finally, the relative high gel level of HIPS C (32.6 wt%) might be related to the very high molecular weight ($\bar{M}_z = 817 \times 10^3$) produced by suspension process.

2.3. Mechanical properties

The stress–strain properties and Izod impact strength of the four rubber-modified materials are summarized in Table 2. HIPS A has the highest impact strength, as well as the lowest tensile strength and modulus. The initial rubber content of HIPS A and the amount of polystyrene grafted and occluded inside the salami-rubber particles gives rise to the highest gel and RPVF, as well as the largest average particle size of the HIPS materials investigated. Comparing HIPS A with HIPS B, both with about 8 wt% of rubber, the difference in impact strength, 141 J/m vs. 85 J/m, is related to the rubber volume fraction, 39.8 wt% vs. 20.7 wt%, respectively.

The two experimental HIPS materials, C and D, have lower rubber content (6 wt%) and correspondingly lower RPVF and rubber particle size than the two commercial materials, which explains, at least in part, their lower Izod impact resistance and elongation to break.

HIPS C has satisfactory Izod strength (78 J/m) and tensile properties, even though it has the smallest rubber particles. It has been generally assumed that large rubber particles initiate crazes more easily than sub-micron ones, with the conclusion that rubber particles smaller than 0.8 μm are much less effective for toughening [5,6]. The two laboratory HIPS have relatively high impact strength despite the fact that both have a significant fraction of sub-micron rubber particles. Keskkula [3], Lavengood [7], Okamoto [8] and Maestrini [9] have reported that good impact resistance can be obtained with an adequate combination of large and sub-micron particles.

The mechanical properties of HIPS D, made by casting, are lower than those of HIPS C (similar d_w and same rubber content), probably because it was not injection molded; the specimens were cut directly from the cast-sheet. As it is well known, mechanical properties of isotropic compression molded HIPS, assumed to be similar to the cast-sheet, are lower than those of the injection molded samples. Injection molded HIPS specimens show considerable anisotropy that gives rise to improvement of the impact strength when compared to specimens with little or no orientation.

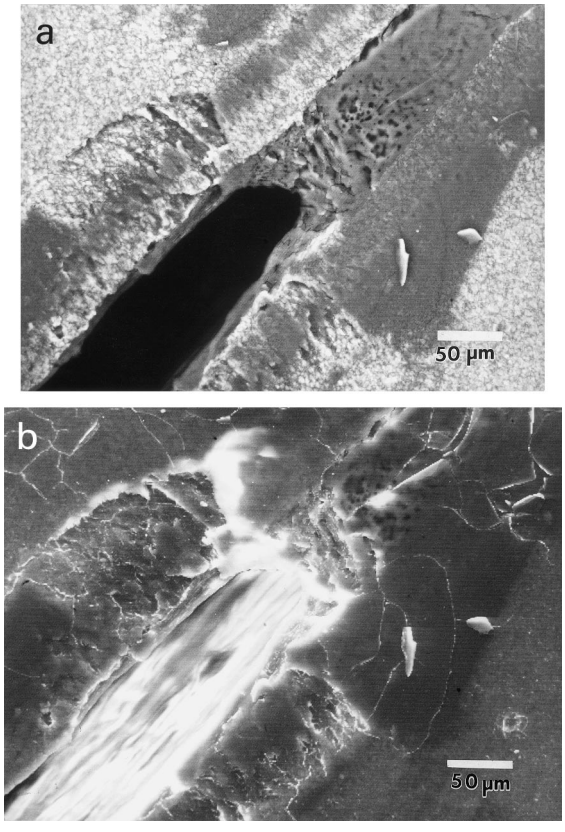

Fig. 1. General overview of an arrested crack tip in HIPS A. Scanning electron photomicrograph of a polished mesa-cut block, stained with OsO_4 and vacuum coated with carbon, using: (a) back-scattering detector; (b) secondary electron detector.

3. Fracture observations

A Dynatup Drop Tower 8200 was used to generate arrested cracks in standard injection molded samples or in specimens from cast sheet. Details about arrested-crack formation have been published elsewhere [20,21]. Typically

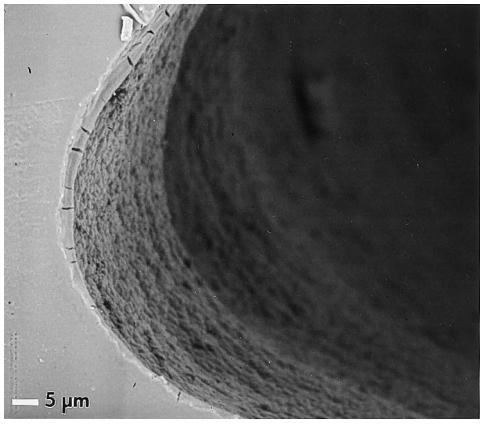

Fig. 2. Arrested crack tip in HIPS B. Scanning electron photomicrograph of a polished mesa-cut block, stained with OsO_4 and vacuum coated with carbon, using back-scattering detector.

the hammer was dropped only 2–6 cm to produce a crack without causing a complete failure. The internal morphology of the osmium tetroxide stained rubber phase was characterized by TEM, using a Jeol CX200 with an accelerating voltage of 120 kV. A Zeiss DSM 940 A scanning electron microscope (SEM) was used to generate complementary information about the crack tip and the associated plastic zone.

A general overview of the crack tip in HIPS A, as viewed by SEM is shown in Fig. 1(a) and (b). Using back-scattered electrons, the crack appears black as seen in Fig. 1(a). The shape of the crack tip is blunted with a width of about 50 μm. As seen from both photomicrographs there is an interesting plastic region, ahead of the crack tip. Several micro-cracks with a width of a few microns and cavities (black zones) are located in this mass right ahead the crack tip (also note Fig. 2). This plastic region, precursor of the crack, is more than 250 μm long. In Fig. 1(b) the same crack tip is shown, but now viewed by secondary electrons to observe deeply inside the structure of the void-crack. The crack-walls appear bright in Fig. 1(b). High matrix orientation is noticed as a set of parallel fibers probably caused by yielding of the polystyrene matrix towards the fracture direction.

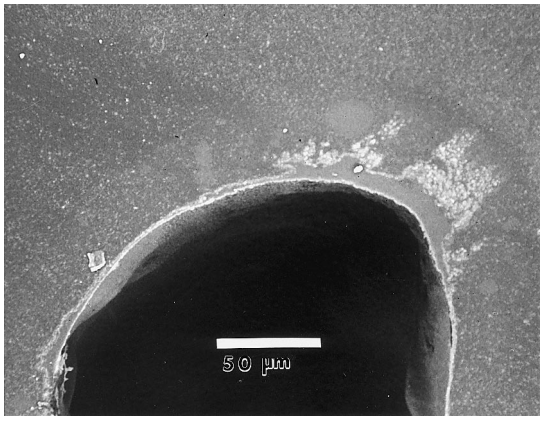

Fig. 3. Arrested crack tip in HIPS D made by mass casting. Scanning electron photomicrograph of a polished mesa-cut block, stained with OsO_4 and vacuum coated with carbon, using back-scattering detector.

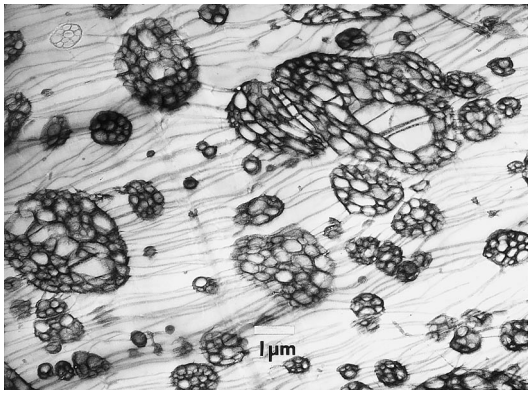

Fig. 4. Network of crazing in HIPS A. Transmission electron photomicrograph under bright field about 20–50 μm from the crack.

The crack tip in HIPS B, as viewed by SEM, has a blunted shape, as seen in Fig. 2. The width of the crack tip is of about 60 μm. Some micro-cracks can be observed near the crack borders and the walls of the crack (polystyrene matrix) appear to be oriented or structured. A general overview of the crack tip, by SEM, is shown in Fig. 3 for HIPS D (small rubber particle size, $\bar{d}_w = 0.6$ μm).

3.1. Region around the crack

In order to develop more details about the toughening of HIPS, TEM observations were made on ultra-thin sections from the fracture zone. Massive crazing was detected for all the materials studied. Typical TEM photomicrograph for HIPS A, in Fig. 4, reveal the crazing network formed over a very wide area of roughly 200 to 400 μm around the arrested crack. A number of crazes are associated with a single rubber particle. All of the rubber particles, even the sub-micron ones (of about 0.3 μm), seem to be connected by one or multiple crazes. The observed crazes are in a plane

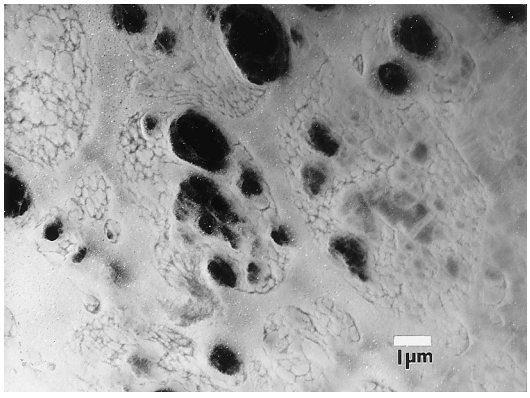

Fig. 5. Transmission electron photomicrograph of a highly deformed zone in HIPS A, stained with OsO_4, slightly away from the crack, where cavitation inside the salami-type rubber particles is shown under dark field.

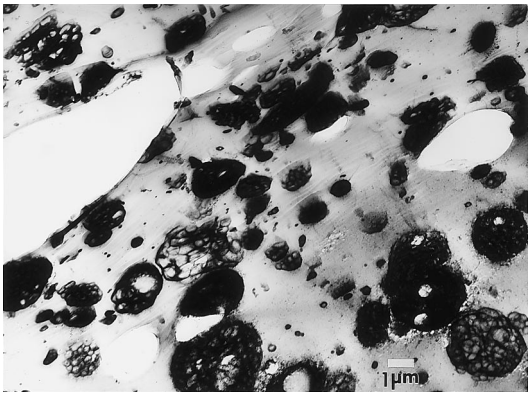

Fig. 6. Transmission electron photomicrograph of a highly deformed zone in HIPS B, stained with OsO_4, slightly away from the crack tip, where a dilatation band and matrix voiding are observed under bright field.

most frequently parallel to the crack direction. Some crazes are also observed in the occluded polystyrene within the rubber particles as seen for the largest particle in Fig. 4.

Highly damaged (cavitated) rubber particles are observed near the crack of HIPS A, as seen by dark filed TEM in Fig. 5. This kind of voiding, inside the salami-type rubber particles, seems to be due to an interfacial failure at the rubber membrane and the polystyrene occlusions leading to a destruction of the particle beyond the single occlusion, i.e. formation of a large cavity.

3.2. Region ahead of the crack tip

The region just ahead of the crack was studied by TEM using ultra-thin sections. For the four HIPS materials, two types of deformation-bands are observed. The term of "dilatation band" is used to denote a zone which has extensive cavitation associated with some elongation of the rubber particles; while the term "shear-band" is used to designate a more narrow volume where the rubber particles are highly elongated, with "S" or "tear-drop" shape.

Fig. 6 is a photomicrograph of HIPS B by TEM bright field showing a dilatation band. The width of the dilatation band is about 10 μm. Some rubber elongation is noticed near the band. Three different types of cavitation and debonding are detected: (1) in the interface occlusions–rubber inside the salami particles, (2) in the interface polystyrene–rubber particles and (3) in the polystyrene matrix.

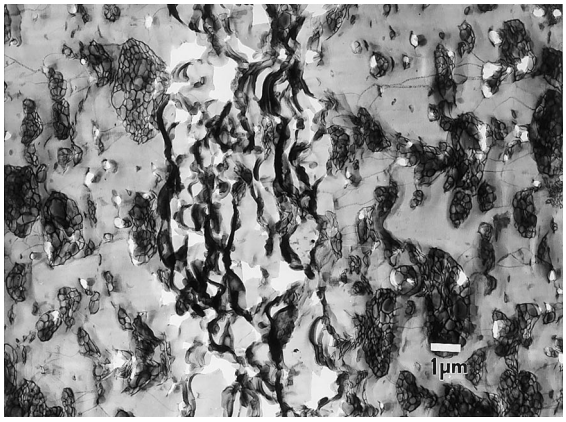

Fig. 7. Shear bands in HIPS A. Transmission electron photomicrograph of a deformed zone slightly ahead of the crack tip. Highly deformed particles with "S" shape and interfacial debonding are in evidence.

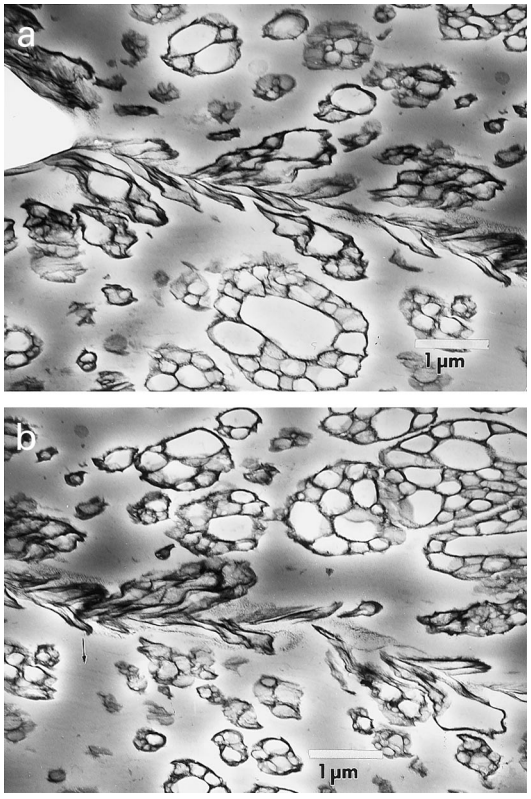

Fig. 8. Shear band in HIPS C. Transmission electron photomicrograph, just ahead of the crack tip, where a narrow shear band, crazing and cavitation within the rubber membrane are noticed: (a) origin of the shear band; (b) continuation of the shear band, arrow indicates the crazes that form parallel to the shear band.

Fig. 7 presents a general overview of a shear-band in HIPS A. The shear-band is lighter than the rest of the section. It is about 4 μm wide and more than 50 μm long. Along the shear-band, the rubber particles are highly elongated having "S" shape. More spherical rubber particles are observed in the darker section of the picture, where some crazing is apparent. In this region two cavitation processes are observed: (1) failure or debonding in the rubber-matrix interface and (2) interfacial failure inside the salami-rubber particle. It is interesting to note that crazing, yielding and cavitation are apparent simultaneously during the fracture of HIPS A.

A shear-band (more than 50 μm long and about 2 μm wide) in HIPS C is shown partially in Fig. 8(a) and (b). Fig. 8(a) shows a micro-crack or a void where the shear band may have started, while Fig. 8(b) shows a continuation of the same band. The rubber particles are highly deformed towards the center of the band, showing a "tear-drop" shape, apparently caused by local shear yielding of the polystyrene

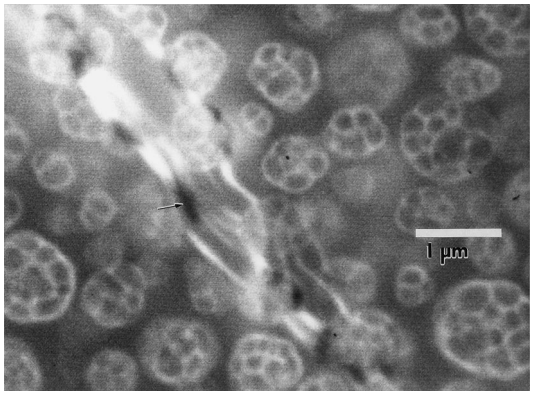

Fig. 9. Dilatation bands in HIPS D. Scanning electron photomicrograph, just ahead of the crack tip, where several dilatation bands are in evidence as crack precursors.

matrix. Thus, the rubber particles seem to flow only partially towards the center of the shear-band producing the "tear-drop" shape. Very fine crazes appear parallel to the shear band. Cavitation is constrained to small holes within the rubber membrane of the particles. These photomicrographs show clear evidence of a narrow shear-band just ahead of the crack tip.

In relation to the mechanical properties, HIPS Awith the highest impact strength (Table 2) is able to generate wider shear-bands of 4–6 μm width. The rubber particles can be deformed to "S" shape. In contrast, HIPS C has lower impact strength and shear bands of 2 μm width. The rubber particles are only partially elongated.

Fig. 9 shows a SEM photomicrographs of HIPS D. A cluster of dilatation bands (bright lines) of more than 30 μm long is observed. In a lower magnification photomicrograph the cluster of bright lines may be judged to be as wide as 6 μm. Some rubber particle deformation is noticed along the bands while in the surrounding area, the particles retain their spherical shape. Several cavities or micro-cracks (darker areas) are located along the shear-bands, as indicated by the arrow. These bands are the precursors of the crack. For the arrested crack in HIPS D, using specimens that are substantially isotropic, there is also evidence of yielding associated with cavitation or debonding at the interface of polystyrene-matrix and the rubber particles.

4. Conclusions

The study of HIPS samples with arrested cracks formed under impact loading using electron microscopy has revealed a complex combination of deformation processes. Extensive crazing is observed in most of the studied sections, but several types of cavitation along with apparent narrow shear and dilatation-bands have been observed just ahead of the crack tip. According to Lazzari and Bucknall [15,16] and Schirrer et al. [19] particle cavitation is a prerequisite for shear yielding of the matrix under the severe conditions of the notched impact test. Our direct TEM and SEM evidences are in accord with this.

The representation of Fig. 10 is consistent with the observations for all the HIPS materials studied here which contain different amounts of rubber, average particle sizes and rubber-crosslinking level. The crack tip has a blunted shape with a width from 60 to 100 μm. Just ahead of the

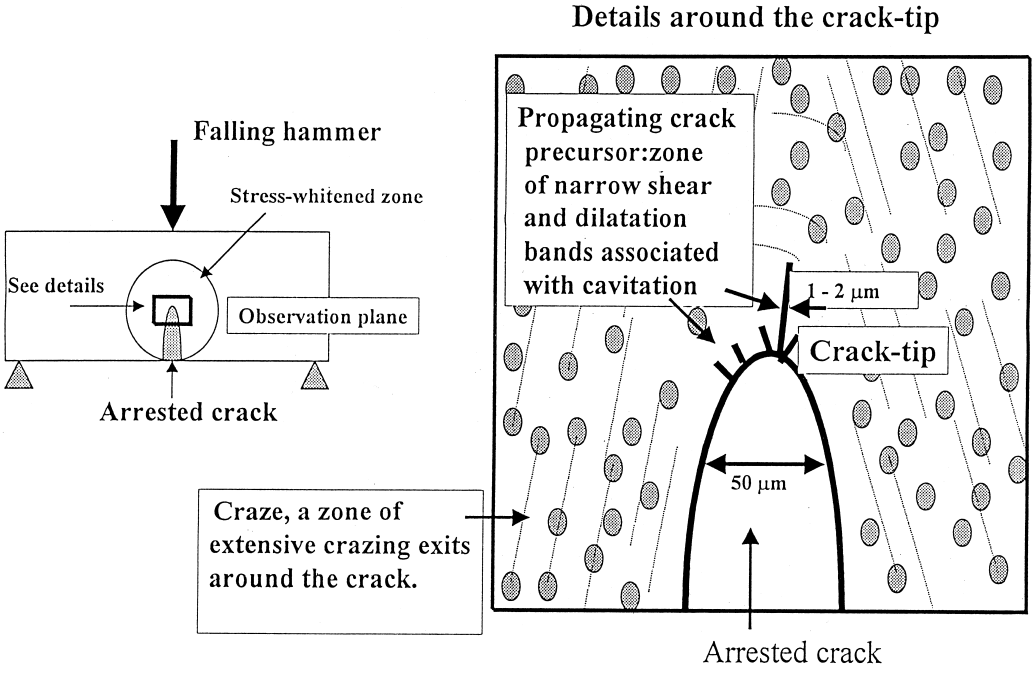

Fig. 10. Schematic of the area near an arrested crack in HIPS.

crack tip, some nascent micro-cracks, shear and dilatation bands are observed, leading to an expanded highly stressed region. This zone represents the crack-precursor. The rest of the section shows extensive crazing. Previously, stress whitening and deformation of HIPS has been attributed mainly to crazing. In this work direct evidence of plastic deformation (yielding) associated with several types of cavitation, are demonstrated in a narrow band of about 2 μm just ahead the crack tip.

There appear to be three types of cavitation in the stress-whitened fracture zone: (1) cavitation as small voids inside the membranes of the rubber particles; (2) large voids at the interface between rubber particles and the matrix, and (3) interfacial cavities between the salami structure of the rubber and the polystyrene occlusions. Furthermore, some voids seem not to be associated with any of the rubber particles.

In subsequent works we will apply this crack tip methodology to rubber-toughened styrene–methyl methacrylate copolymers, to study the effect of the MMA content on the fracture mechanism.

Acknowledgements

We gratefully acknowledge the support of Group Resistol-Mexico for financing the sabbatical year of Dr Leonardo Rios Guerrero.

References

[1] Bucknall CB. Toughened plastics, London: Applied Science Publishers, 1977.
[2] Keskkula H, Schwarz M, Paul DR. Polymer 1986;27:211.
[3] Keskkula H. In: Riew CK, editor. Adv Chem Series 222, Washington: American Chemical Society, 1989 p. 289.
[4] Dagli G, Argon AS, Cohen RE. Polymer 1995;36:2173.
[5] Piorkowska E, Argon AS, Cohen RE. Macromolecules 1990;23:3838.
[6] Donald AM, Kramer EJ. J Appl Polym Sci 1982;27:3729.
[7] Lavengood RE. US Pat 4 214 056. July 22, 1980 (to Monsanto Chem. Co.)
[8] Okamoto Y, Miyagi H, Mitsui S. Macromolecules 1993;26:6547.
[9] Maestrini C, Monti L, Kausch HH. Polymer 1996;37:1607.
[10] Bubeck RA, Buckley DJ, Kramer EJ, Brown HR. J Mater Sci 1991;26:6249.
[11] Bucknall CB, Karpodinis A, Zhang XC. J Mater Sci 1994;29:3377.
[12] Dompas D, Groeninckx G. Polymer 1994;35:4743.
[13] Fond C, Lobbrecht A, Schirrer R, Int J. Fracture 1996;77:141.
[14] Magalhaes AML, Borggreve RJM. Macromolecules 1995;28:5841.
[15] Lazzari A, Bucknall CB. J Mater Sci 1993;28:6799.
[16] Lazzari A, Bucknall CB. Polymer 1995;15:2895.
[17] Van der Sanden MC, Meijer HE, Lemstra PJ. Polymer 1993;34:2148.
[18] Gilbert DG, Donald AM. J Mater Sci 1986;21:1819.
[19] Schirrer R, Fond C, Lobrecht A. J Mater Sci 1996;31:6409.
[20] Kayano Y, Keskkula H, Paul DR. Polymer 1997;38:1885.
[21] Hale W, Keskkula H, Paul DR. Polymer 1999;40:3353.
[22] Vu-Khanh T. Polymer 1988;29:1979.
[23] Sue HJ. Polym Eng Sci 1991;27:270.
[24] Majumdar B, Keskkula H, Paul DR. J Polym Sci, Part B: Polym Phys 1994;32:2127.
[25] Sue HJ. J Mater Sci 1992;27:3098.
[26] Parker DS, Sue HJ, Huang J, Yee AF. Polymer 1990;31:2267.